**Supporting Information**

# Boosted photochromic properties by carbon dots based on Förster resonance energy transfer

Liqiang Kuang,[a] Pengnian Shan,[a] Keyi Chen,[a] Xiaoyang Zhou,[a] Lijing Wang,[c] Weilong Shi,[a]* Chunsheng Li,[d]* Yan Yan,[b]*

[a] *School of Material Science and Engineering, Jiangsu University of Science and Technology, Zhenjiang, Jiangsu 212114, PR China;*

[b] *School of Chemistry & Chemical Engineering/Research Center of Fluid Machinery Engineering and Technology, Jiangsu University, Zhenjiang, 212013, China;*

[c] *Henan Engineering Center of New Energy Battery Materials, College of Chemistry and Chemical Engineering, Shangqiu Normal University, Shangqiu 476000, China;*

[d] *Key Laboratory of Advanced Electrode Materials for Novel Solar Cells for Petroleum and Chemical Industry of China School of Chemistry and Life Sciences, University of Science and Technology, Suzhou, Jiangsu Province, 215009, PR China.*

**Corresponding authors' E-mail: shiwl@just.edu.cn (W. Shi), lichsheng@163.com (C. Li) and dgy5212004@163.com (Y. Yan).*

## 1. Materials

3-amino-1, 2, 4-triazole ($C_2H_4N_4$), Potassium chloride (KCl), Potassium hydroxide (KOH), Triethanolamine (TEOA), 1, 2-Dichloroethane ($C_2H_4Cl_2$) Polymethyl methacrylate ($C_{14}H_{22}O_2$) and N, N-Dimethylformamide ($C_3H_7NO$) were purchased from McLean Chemical Reagent Co, Ltd. All chemicals used in the experiment were of analytical grade and required no further purification.

## 2. Synthesis of CDs powder

Carbon dots (CDs) were synthesized via a typical electrochemical exfoliation method. Briefly, two high-purity graphite rods were sequentially cleaned with ethanol and deionized water, and then immersed in a beaker containing 100 mL of ultrapure water, serving as the anode and cathode, respectively. The interelectrode distance was maintained at approximately 2 cm. A constant direct current (DC) voltage of 30 V was applied using a regulated power supply, while the reaction system was continuously magnetically stirred to promote efficient exfoliation. During the electrochemical oxidation process, the initially colorless solution gradually turned into a dark black dispersion,

indicating the formation of carbon dots. After continuous electrolysis for 10 days, the reaction was terminated. The resulting suspension was filtered through quantitative filter paper to remove residual graphite particles and large aggregates. Finally, the filtrate was collected and freeze-dried for 48 h to obtain the as-prepared CDs powder.

## 3. Preparation of CDs/HC-$C_3N_5$ photochromic film

First, 0.8 g of CD/HC-$C_3N_5$ was dispersed in 4 mL of N, N-dimethylformamide (DMF), with 2 mL of TEOA solution subsequently added, followed by 2 h of stirring and 30 min of ultrasonication to achieve a homogeneous dispersion. Simultaneously, 8 g of polymethyl methacrylate (PMMA) was dissolved in 16 mL of 1,2-dichloroethane under continuous stirring at room temperature for 8 h until completely dissolved. The two solutions were mixed at a volumetric ratio of 1:4, stirred at room temperature for 1 h to obtain the photochromic film precursor, and subsequently spin-coated onto a pretreated glass slide. A 500 μL aliquot of the composite precursor was deposited at the center of the substrate, spin-coated at 1000 rpm for 60 s, left to stand at room temperature for 30 min, and subsequently subjected to thermal treatment in a vacuum drying oven at 50 °C for 2 h, before finally being detached from the substrate to obtain the CDs/HC-$C_3N_5$ photochromic film.

## 4. Characterizations

X-ray diffraction (XRD) patterns of samples were acquired from an XRD diffractometer (XRD, Apex II, Bruker X-ray diffractometer) with Cu Kα radiation (40 kV, 30 mA) over a scanning range of 2θ =5-80° at a scanning rate of 8°/min. Fourier transform infrared spectroscopy (FT-IR) was collected from 4000 to 600 $cm^{-1}$ on a Bruker Vertical-70 spectrometer with a resolution of 1 $cm^{-1}$. Transmission electron microscopy (TEM), high-resolution HRTEM images, and EDX images were obtained with FEI-TecnaiTM G2F30 and 200 kV field firing guns. X-ray photoelectron spectroscopy (XPS) was measured using an ESCALAB 250Xi instrument (K-Alpha, Thermo Fisher Scientific) with a calibration standard of 284.6 eV, and the XPS spectra were fitted by XPSPEAK41 software. Photoluminescence (PL) spectra were obtained via luminescence spectrometer (RF-5301PC, exciting sample at wavelength 365 nm). The UV-Vis diffuse reflectance spectra of light under air conditions for different times were studied by a miniature fiber optic spectrometer Maya 2000Pro (200-1100 nm).

## 5. Evaluation of the photochromic performance

Photochromic experiments on CDs/HC-$C_3N_5$ films were carried out under ultraviolet (UV) irradiation, and a 300 W Xenon lamp with a 320 nm cut off filter was used as the UV light source for the photochromic experiments. The color change that occurs in the film during the coloring-bleaching process can be captured by a digital camera. The color change of the films under UV irradiation and darkness can be easily quantified by image analysis using the Commission Internationale de L'Eclairage (CIE) $L^*a^*b^*$ color space [1]. Furthermore, the remaining degree of color (RC%) was utilized to evaluate the bleaching degree at specific time intervals with using the equation as follows (equation 1):

$$RC\% = \left(A_t - A_0 / A_\infty - A_0\right) \times 100\% \tag{1}$$

where $A_t$, $A_\infty$ and $A_0$ represent the UV–vis absorbances of the sample at 480 nm at bleaching time, before the bleaching and before the irradiation, respectively [2].

## 6. Calculation of FRET efficiency and Förster distance ($R_0$)

The critical transfer radius between the donor and acceptor with energy transfer efficiency of 50% is defined as the Forster distance ($R_0$)[3, 4] and the $R_0$ of the CDs and HC-$C_3N_5$ can be calculated according to the equations:

$$J(\lambda) = \frac{\left[\int_0^\infty F_D(\lambda)\varepsilon_A(\lambda)\lambda^4 d\lambda\right]}{\left[\int_0^\infty F_D(\lambda)d\lambda\right]} \tag{2}$$

$$R_0^6 = 8.79 \times 10^{-15}\left[k^2 n^{-4}\Phi_D J(\lambda)\right] \tag{3}$$

where $F_D(\lambda)$ is the area-normalized emission spectrum of donor, $\varepsilon_A(\lambda)$ is the molar absorption spectrum of the acceptor in $M^{-1}$ $cm^{-1}$ , $k^2$ is the wavelength in nm, $k^2$ is the orientation factor (the value of $k^2$ is 2/3 due to dynamic averaging of the donor–acceptor systems), $\Phi_D$ is the quantum yield of the donor, and n is the refractive index of the surrounding medium.

Furthermore, the FRET efficiency (E) was quantitatively estimated using the donor fluorescence lifetime shortening method:

$$E = 1 - \frac{\tau_{DA}}{\tau_D} \tag{3}$$

where $\tau_D$ and $\tau_{DA}$represent the average fluorescence lifetimes of CDs in the absence and presence of HC-$C_3N_5$, respectively.

## 7. Figures and tables

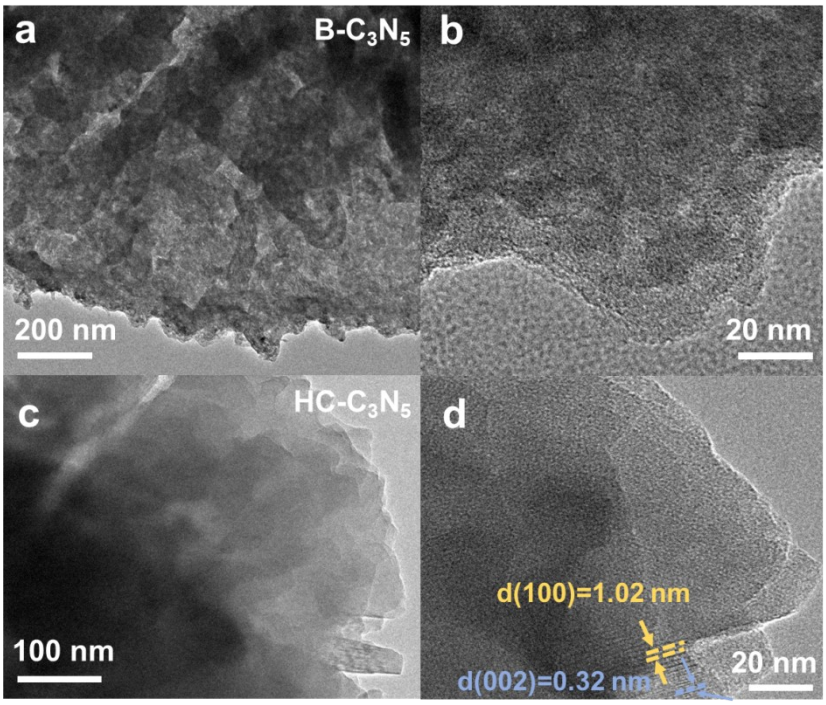


**Fig.S1** TEM/HRTEM images of (a, b) B-$C_3N_5$ and (c, d) HC-$C_3N_5$.

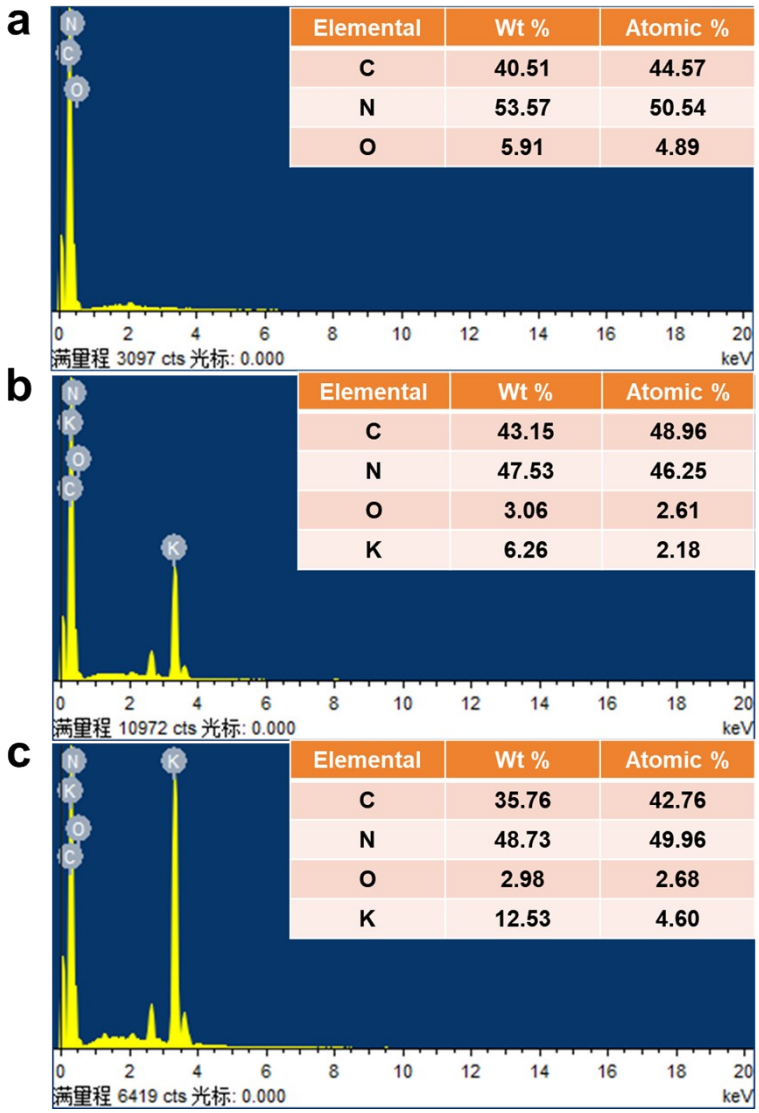


**Fig.S2** EDX spectra of as-prepared (a) B-$C_3N_5$, (b) HC-$C_3N_5$ and (c) CDs/HC-$C_3N_5$ samples.

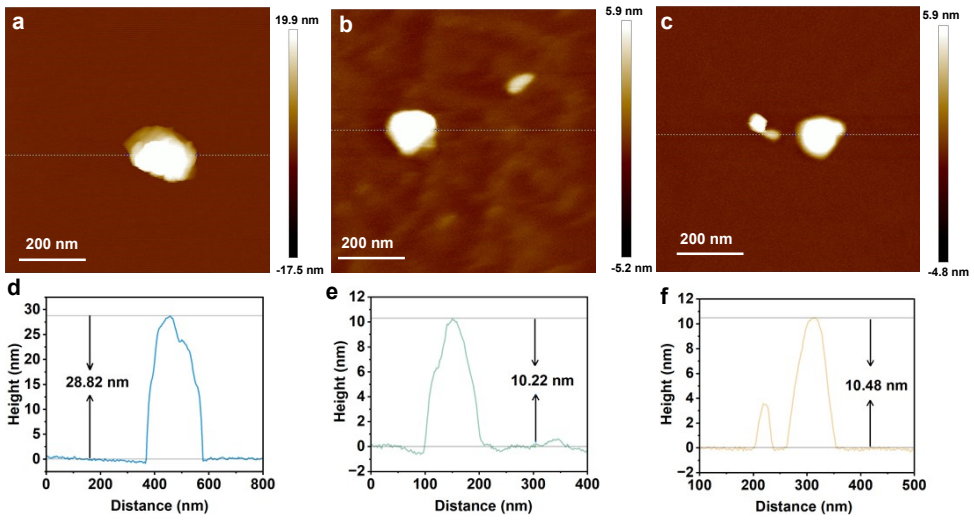


**Fig.S3** AFM images and corresponding height profiles of (a, d) B-$C_3N_5$, (b, e) HC-$C_3N_5$, and (c, f) CDs/HC-$C_3N_5$.

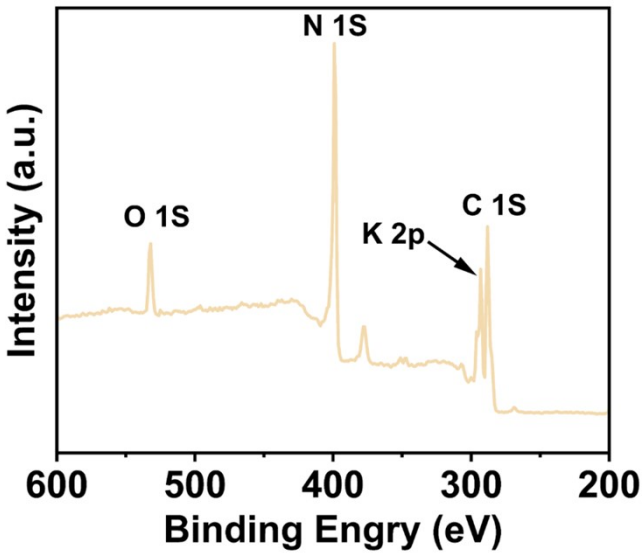


**Fig.S4** XPS survey spectrum of CDs/HC-$C_3N_5$ composite.

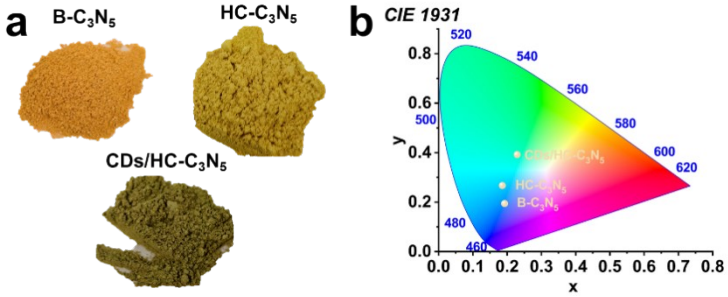


**Fig.S5** (a) Optical photographs of B-$C_3N_5$, HC-$C_3N_5$ and CDs/HC-$C_3N_5$ and (b) corresponding CIE color coordinates.

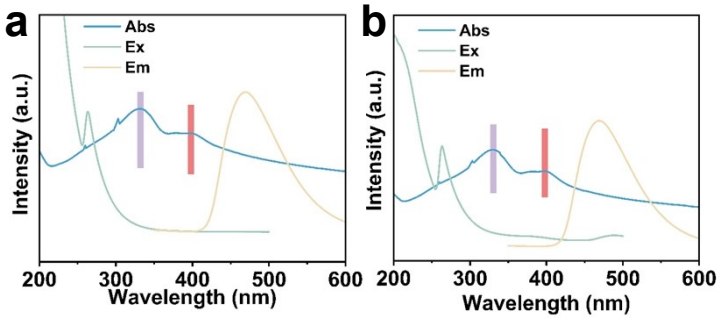


**Fig.S6** UV–Vis absorption, fluorescence excitation and emission spectra of (a) B-$C_3N_5$ and (b) HC-$C_3N_5$ powder.

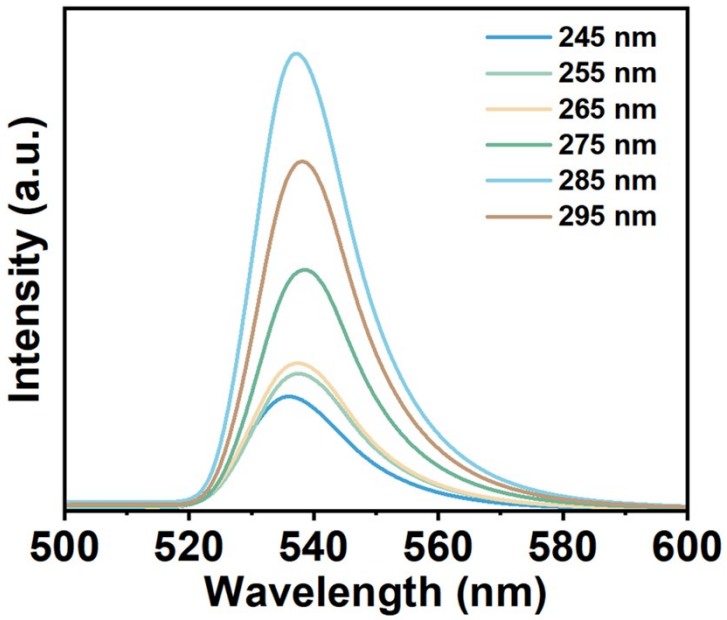


**Fig.S7** Fluorescence spectra of CDs/HC-$C_3N_5$ powder at different excitation wavelengths.

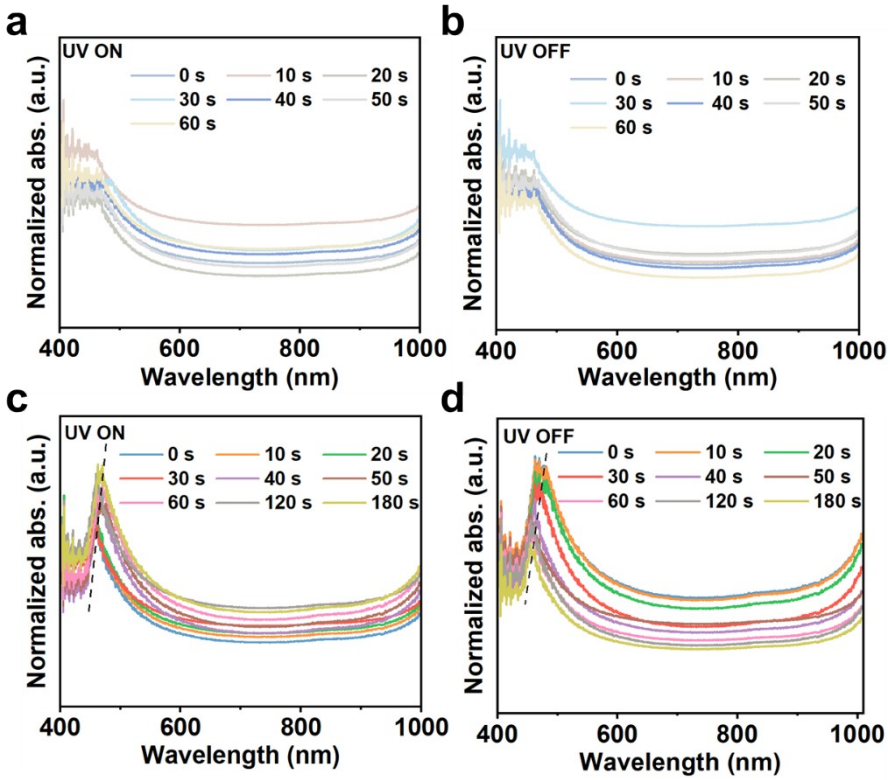


**Fig.S8** Normalized in-situ reflection of (a-b) B-$C_3N_5$ and (c-d) HC-$C_3N_5$ in TEOA solution for coloring and bleaching under the UV irradiation with different time.

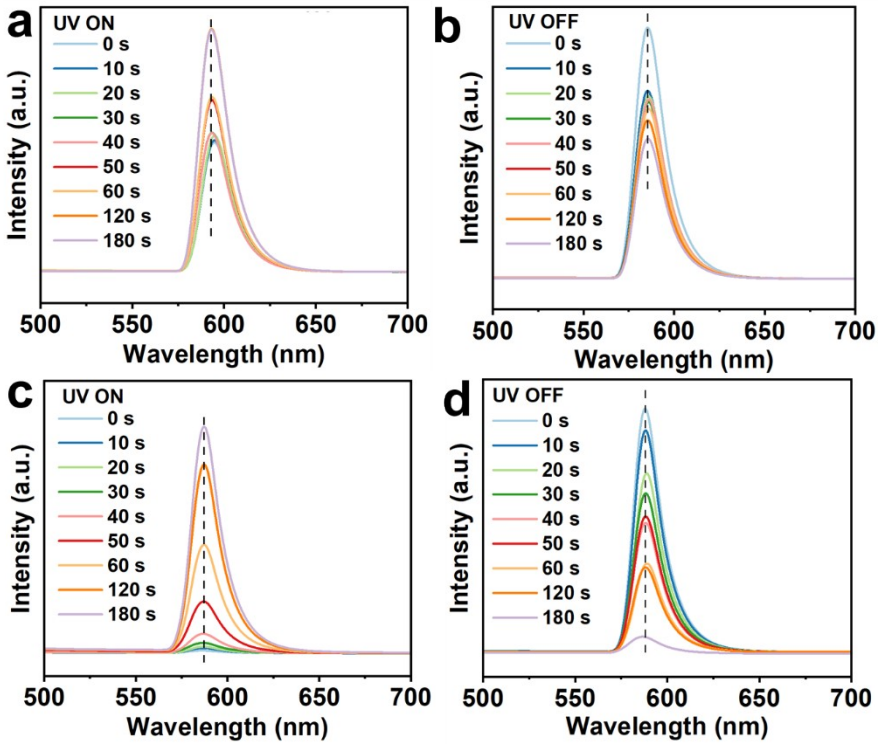


**Fig.S9** PL spectra of (a, b) B-$C_3N_5$ and (c, d) HC-$C_3N_5$ change with irradiation time during coloring and bleaching.

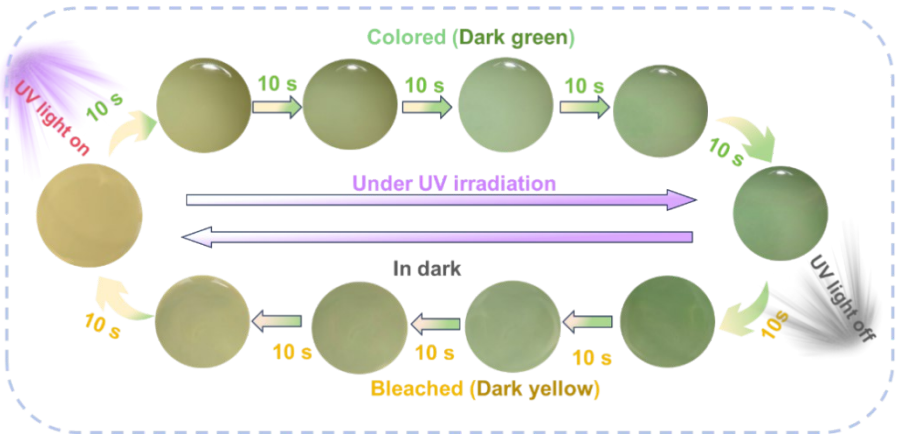


**Fig.S10** Coloring and bleaching processes of CDs/HC-$C_3N_5$ in TEOA solution.

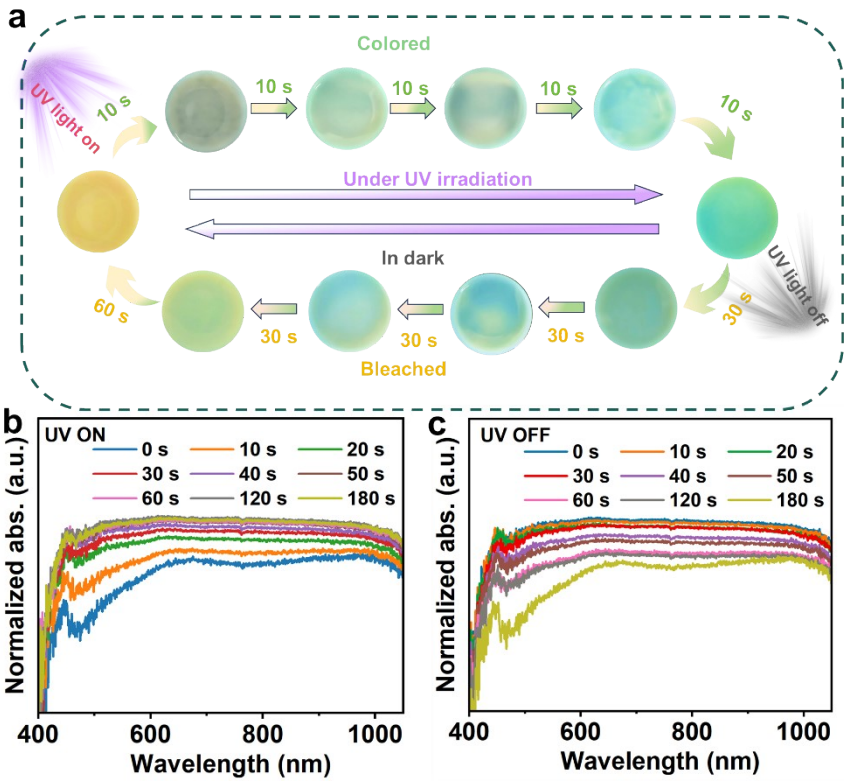


**Fig.S11** (a) Coloration and bleaching processes of CDs/HC-$C_3N_5$ in a TEOA solution under a nitrogen atmosphere. Normalized in-situ reflection of (b) coloring and (c) bleaching under the UV irradiation at different time.

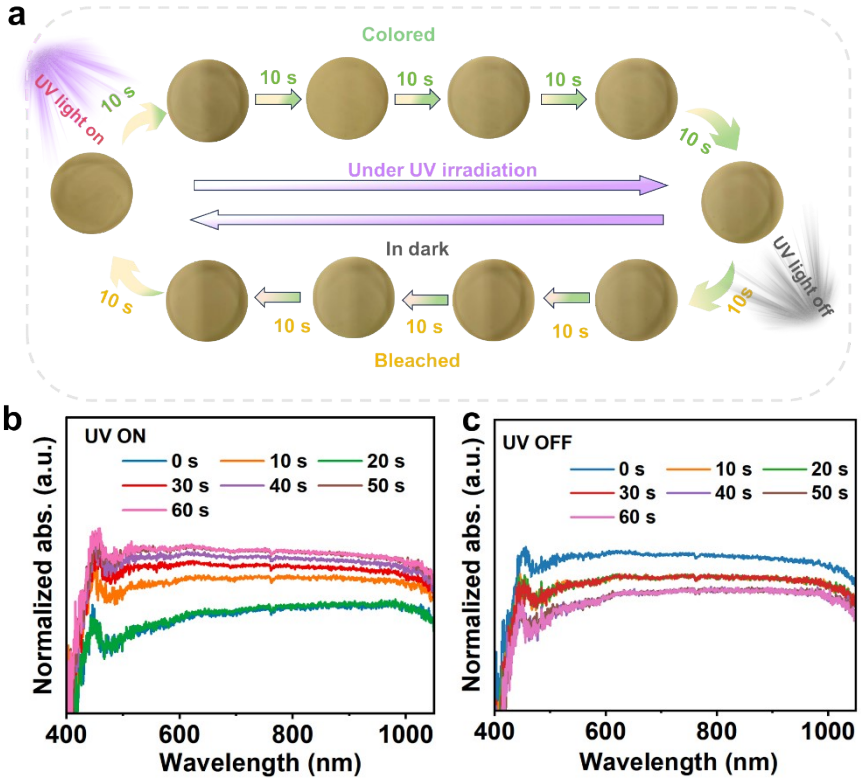


**Fig.S12** (a) Coloration and bleaching processes of CDs/HC-$C_3N_5$ in a pure water. Normalized in-situ reflection of (b) coloring and (c) bleaching under the UV irradiation at different time.

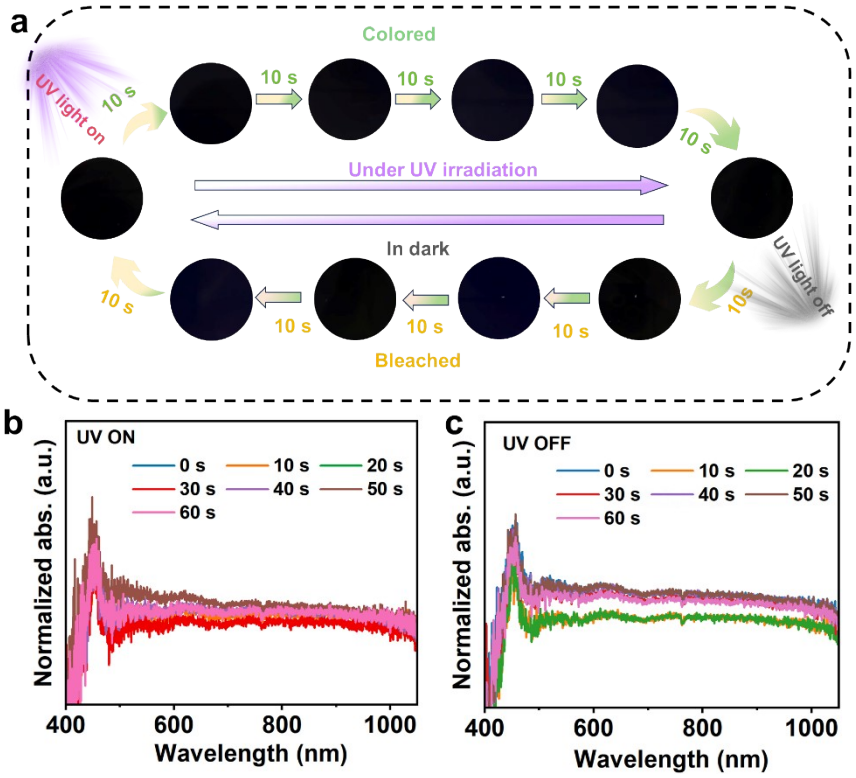


**Fig.S13** (a) Coloration and bleaching processes of CDs in TEOA solution. Normalized in-situ reflection of (b) coloring and (c) bleaching under the UV irradiation at different time.

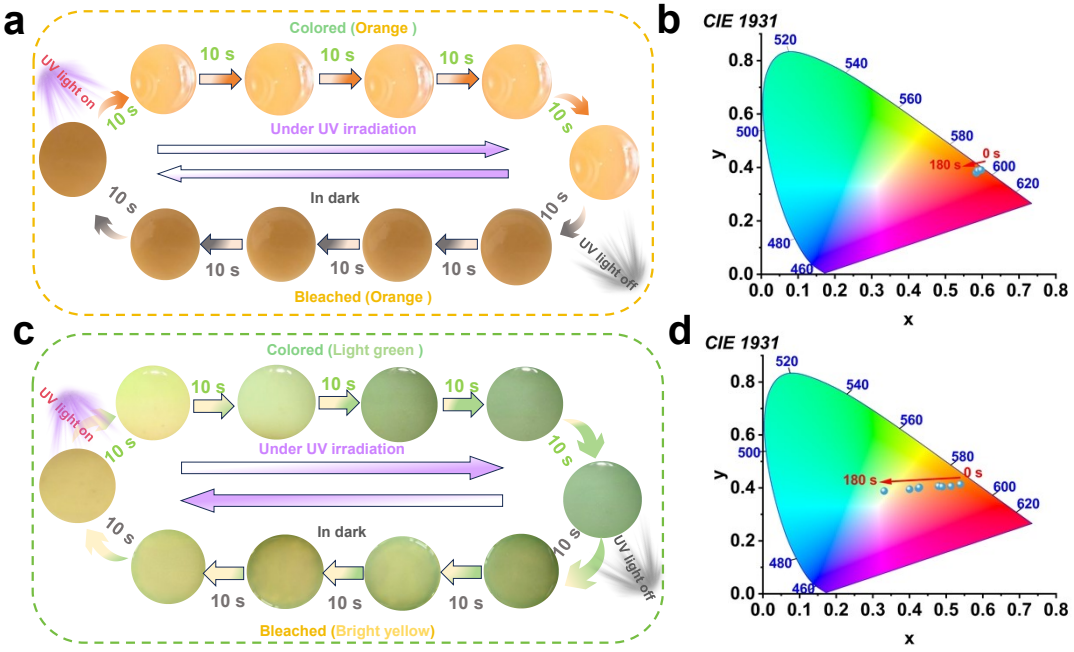


**Fig.S14** Coloring and bleaching processes of (a) B-$C_3N_5$ and (c) HC-$C_3N_5$ irradiated under UV light; CIE colorimetric diagrams of (b) B-$C_3N_5$ and (d) HC-$C_3N_5$.

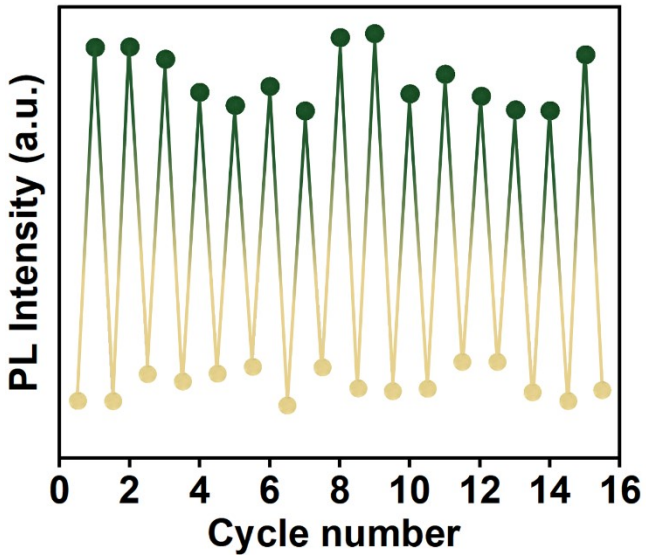


**Fig.S15** Reversibility of the photoactivated (180 s) and deactivated for CDs/HC-$C_3N_5$ material.

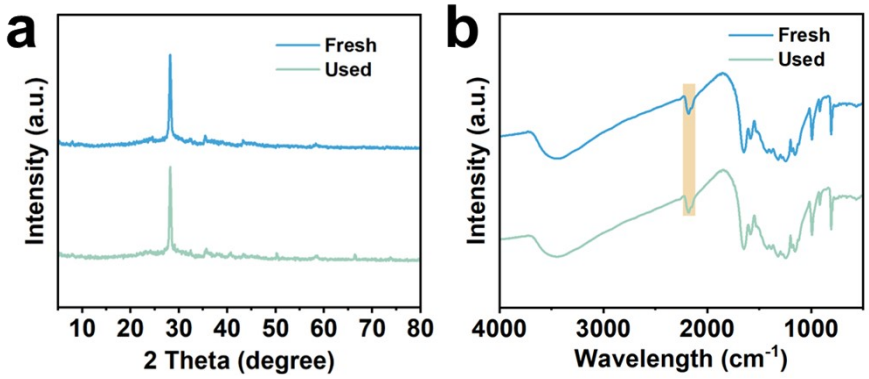


**Fig.S16** (a) XRD patterns and (b) FT-IR spectra of CDs/HC-$C_3N_5$ after multi-cycle photoactivation experiments.

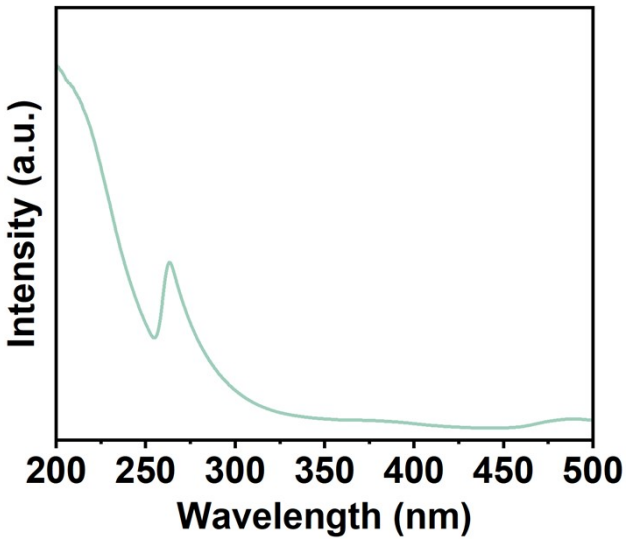


**Fig.S17** Excitation spectrum of the HC-$C_3N_5$ sample.

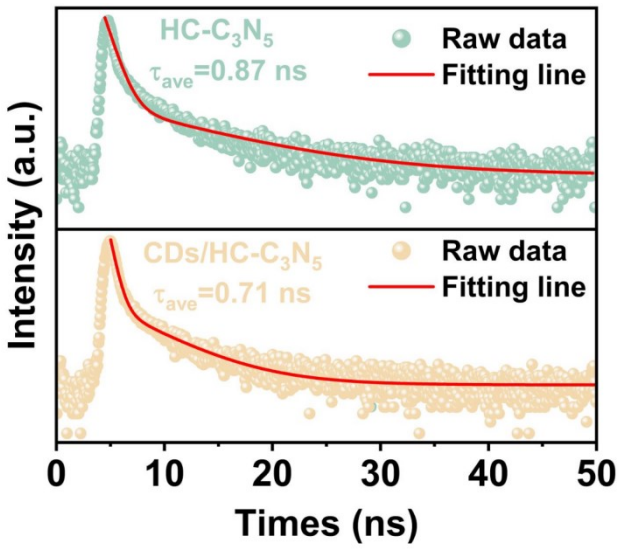


**Fig.S18** TRPL decay curves of HC-$C_3N_5$ and CDs/HC-$C_3N_5$.

**Table S1** Comparison of photochromic performance between the CDs/HC-$C_3N_5$ composite and other representative photochromic systems.

| Material System | Mechanism | Response Time | Recovery Time | Cycling Stability | Color Transition | Ref. |
|---|---|---|---|---|---|---|
| CDs/HC-$C_3N_5$ | FRET-assisted $e^-$ storage | 50 s | 180 s | Excellent | Dark yellow to green | This work |
| Paper/$WO_3$/PDMS | Photoinduced redox reaction | 180 s | < 30 min | Excellent | Colorless to dark blue | 5 |
| $WO_3$ nanoflowers fabric | Photoinduced redox reaction | 120 s | 5 min | Excellent | Colorless to dark blue | 6 |
| HCCN CNFs | Hot-electron-induced LSPR | a couple of minutes | tens of hours | Excellent | Yellow to blue | 7 |
| F-PCN | Free radical anions due to redox reactions | 20 min | 90 min | Good | Yellow to blue | 8 |
| SP@polyPFC-1-G | Photoisomerization and fluorescence resonance energy transfer | 3 min | 5 min | Good | Yellow to dark brown | 9 |
| XG/PMMA | Reversible isomerization | 30 min | 30 min | Good | Pink to Orange | 10 |
| CMC/CDs/Ammonium molybdate Hydrogel | Dual response of photochromic and fluorescent switching | 6 min | 25 min (60℃) | Good | Light Yellow to Dark Green | 11 |

**Table S2** Parameters and quantitative calculation of FRET between CDs and HC-$C_3N_5$.

| Parameter | Value | Source /Determination |
|---|---|---|
| Donor emission maximum (λ) | 480 nm | Fig.3a |
| Acceptor absorption range | 400–550 nm | Fig.3a |
| Donor quantum yield ($\Phi_D$) | 0.18-0.22 | Typical CDs value (electrochemical CDs, literature[12, 13]) |
| Refractive index of medium (n) | 1.4 | - |
| Dipole orientation factor ($k^2$) | 2/3 | Randomly orientated dipoles |
| Normalized donor emission ( $\int_0^\infty F_D(\lambda)d\lambda$ ) | 1 | From CDs PL spectrum (normalized) |
| Acceptor absorption ($\varepsilon_A(\lambda)$) | $1.0\times10^4$ $M^{-1}$ $cm^{-1}$(450 nm) | HC-$C_3N_5$ absorption |
| Spectral overlap integral | (2.1-2.5) × $10^{15}$ | Calculated value |
| Donor lifetime (without acceptor $\tau_D$) | 0.87 ns | Fig.S18 |
| Donor lifetime (with acceptor $\tau_{DA}$) | 0.71 ns | Fig.S18 |
| Förster distance ($R_0$) | 3.6-4.0 nm | Calculated value |
| FRET efficiency (E) | 35-40 % | Calculated value |

**Table S3** Photochromic anti-counterfeiting photocode book.

| Number | Letter | Number | Letter | Number | Letter |
|---|---|---|---|---|---|
| 000 | A | 100 | X | 200 | S |
| 001 | B | 101 | K | 201 | T |
| 002 | C | 102 | L | 202 | U |
| 010 | D | 110 | M | 210 | V |
| 011 | E | 111 | N | 211 | W |
| 012 | F | 112 | O | 212 | J |

| | | | | | |
|---|---|---|---|---|---|
| 020 | G | 120 | P | 220 | Y |
| 021 | H | 121 | Q | 221 | Z |
| 022 | I | 122 | R | 222 | ! |

## References


1. M. R. Luo, G. Cui and B. Rigg, *Color Res. Appl.*, 2001, 26, 340-350.
2. W. Wu, M. Ni, Q. Feng, Y. Zhou, Y. Cui, Y. Zhang, S. Xu, L. Lin, M. Zhou and Z. Li, *Mater. Des.*, 2024, 238 112613.
3. Y. Zheng, K. Arkin, Y. Bei, X. Ma and Q. J. M. Shang, *Matter*, 2023, 6, 4339-4356.
4. Y.-C. Liang, Q. Cao, K.-K. Liu, X.-Y. Peng, L.-Z. Sui, S.-P. Wang, S.-Y. Song, X.-Y. Wu, W.-B. Zhao and Y. Deng, *ACS Nano*,2021, 15, 16242-16254.
5. T. Chen, X. Mai, Y. Li, T. Wang, R. Gong, F. Chen, H. Huang, Z. Yan and F. Wang, *Chem. Eng. J.*, 2024, 499, 155999.
6. T. Chen, B. Xu, M. Zhu, J. Zhang, W. Sun and J. Han, *Chem. Eng. J.*, 2024, 490, 151804.
7. H. Cheng, W. Sun, Y. Lu, H. Li, W. Su, J. Zhang, T. Guo, F. Li, P. S. Francis and Y. Zheng, *Cell Rep. Phys. Sci.,* 2021, 2 (8).
8. R. Mann and D. Khushalani, *J. Mater. Chem. A*, 2023, 11, 20601-20607.
9. Y. Gao, Q. Li, H. Cai, C. Wu, Y. Wei, Y. Yang *ACS App. Mater. Interfaces*, 2025, 17, 8127-8135.
10. H. Wu, W. Wu, L. Hu, J. Zhu, Q. Li, Y. Gao, Y. Wei, G. Jiang and Y. Yang, *Chem. Eng. J.*, 2023, 469, 143781.
11. Y. Zhong, Z. Wang, L. Quan, Y. Wu, D. Hu, J. Cheng, Y. Zheng, *J. Colloid Interface Sci.* 2025, 679, 393-402.
12. B. Wang and S. Lu, *Matter*, 2022, 5, 110-149.
13. H. Liu, X. Zhong, Q. Pan, Y. Zhang, W. Deng, G. Zou, H. Hou and X. Ji, *Coord. Chem. Rev.,* 2024, 498, 215468.